'Warm Cover'- Precursory 'Strong Signals' hidden in the Middle Troposphere for Haze Pollution

Xiangde Xu[1], Wenyue Cai[1, 2, 3], Tianliang Zhao[4], Xinfa Qiu[5], Wenhui Zhu[6], Chan Sun[1], Peng Yan[7], Chunzhu Wang[8], and Fei Ge[9]

[1]State Key Laboratory of Severe Weather (LASW), Chinese Academy of Meteorological Sciences, Beijing, China.

[2]National Climate Center, China Meteorological Administration, Beijing, China.

[3]School of Geographical Science, Nanjing University of Information Science and Technology, Nanjing, Jiangsu Province, China.

[4]Key Laboratory for Aerosol-Cloud-Precipitation of China Meteorological Administration, Nanjing University of Information Science and Technology, Nanjing, Jiangsu Province, China.

[5]School of Applied Meteorology, Nanjing University of Information Science and Technology, Nanjing, Jiangsu Province, China.

[6]Beijing Institute of Applied Meteorology, Beijing, China.

[7]Meteorological Observation Center, China Meteorological Administration, Beijing, China.

[8]Training Center, China Meteorological Administration, Beijing, China.

[9]School of Atmospheric Sciences/Plateau Atmosphere and Environment Key Laboratory of Sichuan Province/Joint Laboratory of Climate and Environment Change, Chengdu University of Information Technology, Chengdu, Sichuan Province, China.

Correspondence: Wenyue Cai (caiwy@cma.gov.cn) and Tianliang Zhao (tlzhao@nuist.edu.cn)

Abstract. Eastern China (EC), located in the downstream region of Tibetan Plateau (TP), is a large area with frequent haze pollution. In addition to air pollutant emissions, meteorological conditions were a key 'inducement' for air pollution episodes. Based on the study of the Great Smog of London in 1952 and haze pollution in EC over recent decades, it is found that the abnormal 'warm cover' (air temperature warm anomalies) in the middle troposphere, as a precursory 'strong signal', could connect to severe air pollution events. The convection and vertical diffusion in the atmospheric boundary layer (ABL) were suppressed by a relatively stable structure of 'warm cover' in the middle troposphere, leading to the ABL height decreases, which was favourable for the accumulation of air pollutants in the ambient atmosphere. The anomalous structure of the troposphere's "warm cover" not only exist in heavy haze pollution on the daily scale, but also provide seasonal, interannual and interdecadal 'strong signals' for frequently occurring regional haze pollution. It is revealed that a close relationship existed between interannual variations of the TP's heat source and the 'warm cover' strong-signal in the middle troposphere over EC. The warming TP could lead to the anomalous 'warm cover' in the middle troposphere from the plateau to the downstream EC region and even the entire East Asian region for air pollution.

1 Introduction

In China, mainly over the region east of 100 °E and south of 40 °N (Tie et al., 2009), $PM_{2.5}$ (particulate matter with an aerodynamic diameter equal to or less than 2.5 μm) has become the primary air pollutant in winter (Wang, et al., 2017). Therefore，in September 2013, the Chinese government launched the China's first air pollution control action plan-'The Airborne Pollution Prevention and Control Action Plan (2013-2017)' (State Council of the People's Republic of China, 2013). By 2017, about 64% of China's cities are still suffering from air pollution, especially Beijing-Tianjin-Hebei region and surrounding areas (Wang et al., 2019; Miao et al., 2019). Then, in July 2018, the Chinese government launched the second three-year action plan for air pollution control, the "blue sky defense plan", which demonstrates China's firm determination and new measures for air pollution control (State Council of the People's Republic of China, 2018). After the implementation of air pollution control action plans, air quality in many regions in China has been significantly improved.

Anthropogenic pollutant emissions and unfavorable meteorological conditions are commonly regarded

53 as two key factors for air pollution (Ding and Liu, 2014; Yim et al., 2014; Zhang et al., 2015). Air pollutants

54 mainly come from surface emission sources, and most of air pollutants are injected from the surface to the

55 atmosphere through the atmospheric boundary layer (ABL) (Quan et al., 2020). The ABL structures are the

56 key meteorological conditions which influences the formation and maintenance of heavy air pollution

57 episodes (Wang et al., 2015; Cheng et al., 2016; Wang et al., 2016; Tang et al., 2016; Wang et al., 2019).

58   Most of the previous studies focused on exploring the impact on the heavy air pollution in Eastern

59 China (EC) from the meteorological conditions in ABL. However, the thermodynamic and dynamic

60 structures of free troposphere can affect the meteorological conditions in ABL (Cai et al., 2020). The

61 convection and diffusion in the ABL are suppressed by a relatively stable structure in the middle

62 troposphere, leading to the ABL height decreases, which was favourable for the formation and persistence

63 of heavy air pollution (Quan et al., 2013; Wang et al., 2015; Cai et al., 2020).

64   This study investigated whether the thermodynamic structure of the troposphere and its intensity

65 changes can be used as a "strong warning signal" for the changes of $PM_{2.5}$ concentrations in heavy air

66 pollution, and whether this strong signal exists in the time scales of seasonal, interannual and interdecadal

67 changes. In order to explore the interaction between the free troposphere and the ABL and the impact on

68 the heavy air pollution in EC, this study extended the meteorological conditions for heavy air pollution

69 from the boundary layer to the middle troposphere. We identify a precursory 'strong signals' hidden in the

70 free troposphere for frequent haze pollution in winter in EC.

71

72 **2 Data and methods**

73 The data used in this study included NCEP/NCAR and ERA-Interim reanalysis data of meteorology, as

74 well as data of surface $PM_{2.5}$ concentration measurement, air temperature observation and L-band sounding,

75   as briefly described as follows:

76   The monthly NCEP/NCAR reanalysis data of meteorology with horizontal resolution of 2.5° of

77   1960-2019 were obtained from the U.S. National Center for Environmental Protection (NCEP,

78   https://www.esrl.noaa.gov/).

79   The daily and monthly ERA-Interim reanalysis data of meteorology with horizontal resolution of 0.75°

80   were derived from the European Center for Medium-range Weather Forecasts (ECMWF,

81   https://www.ecmwf.int/), including air temperature, geopotential height, humidity, wind field and vertical

82   velocity.

83   The hourly $PM_{2.5}$ concentration data during 2013-2019 were collected from the national air quality

84   monitoring network operated by the Ministry of Ecology and Environment the People's Republic of China

85   (http://www.mee.gov.cn/). In addition, we categorized air pollution levels with the surface $PM_{2.5}$

86   concentrations based on the National Ambient Air Quality Standards of China (HJ633-2012) released by

87   the Ministry of Ecology and Environment in 2012 as shown in Table 1.

88   We also used the monthly air temperature of surface observation data during 1960-2014 from 58

89   meteorological observation stations in the plateau area with an altitude above 3000 meters, which were

90   archived from the China Meteorological Information Center (http://data.cma.cn/).

91   Furthermore, the L-band sounding 'seconds-level' data of Beijing from 2010 to 2019 to were used to

92   calculate the height of ABL (Liu and Liang, 2010). The height of ABL top is characterized by the L-band

93   sounding observations at 20:00 (local time is used for this paper). The L-band sounding 'seconds-level'

94   data has been undergone the quality control before analysis (Zhu et al., 2018), and interpolation was

95   implemented in a vertical direction at an interval of 2 hPa. The L-band detection data provided by the

96   China Meteorological Information Center (http://data.cma.cn/) contains several automatic observation

97   meteorological elements with time resolution of 1.2 s and vertical resolution of 8 m. More detail

98   information can be found in Li et al. (2009) and Cai et al. (2014).

99   **Table 1. Air pollution degrees categorized with surface PM$_{2.5}$ concentrations**

| Air pollution degrees	PM$_{2.5}$ concentration ranges
'less-serious' pollution	$75 \mu g \cdot m^{-3} < PM_{2.5} \leqslant 115 \ \mu g \cdot m^{-3}$
'serious' pollution	$115 \ \mu g \cdot m^{-3} < PM_{2.5} \leqslant 150 \ \mu g \cdot m^{-3}$
'more-serious' pollution	$150 \ \mu g \cdot m^{-3} < PM_{2.5} \leqslant 250 \ \mu g \cdot m^{-3}$
'most-serious' pollution	$PM_{2.5} > 250 \ \mu g \cdot m^{-3}$

100

101   **3 Results**

102   **3.1 A precursory 'strong signal' of 'warm cover' in the middle troposphere**

103   In February 2014, a rarely persistent air pollution weather process occurred in EC with severe air pollution

104   in more than 50 cities, with an impact area of 2.07 million km^2. In the Beijing area during February 20–26,

105   2014 the regional average PM$_{2.5}$ concentration exceed the 'most-serious' air pollution level, and with a

106   peak value of up to 456 μg m^{-3}. In addition, the Great Smog of London in 1952 was attributed to the

107   long-lasting and heavy haze pollution under the influence of certain weather systems (Whittaker et al.,

108   2004). To find the precursory 'strong signals' hidden in meteorology for heavy air pollution events, we

109   retrieved the three-dimensional atmospheric dynamic and thermal structures during December in 1952 as

110   well as February in 2014 by analyzing vertical anomalies of meteorology. There were high-pressure

111   systems moved to London as well as Beijing and stagnated over both areas at 500 hPa geopotential

112   height anomalies, as shown in Figs. 1a and 1b. During the heavy air pollution events, a high-pressure

113   system over London as well as Beijing gradually strengthened (Figs. 1c and 1d), and the middle

114   troposphere was characterized by a 'warm cover' with 'upper warming and bottom cooling' anomalies in

115   vertical structure of air temperature (Figs. 1e and 1f).

116   By comparing Figs. 1a and 1b, we found that two persistent heavy air pollution events occurred during

117   the maintenance stage of stable high pressure system. During stagnation of the blocking high pressure

118   system, the strength of the center of the geopotential height anomalies in the stable maintenance region of

119   the blocking exhibited a synchronous response to the 'warm cover' above areas (Figs. 1c–1f). It can be seen

120   that the local atmospheric thermal structure is significantly modulated by the persistent large-scale

121   anomalous circulation. The 'subsidence-induced air temperature inversion' effect of the blocking high

122   pressure system continuously strengthened the 'warm cover' structure in the middle troposphere, which

123   suppressed the vertical diffusion capacity in the atmosphere (Cai et al., 2020). Moreover, it was obvious

124   that 'strong signals' arising from the thick 'warm cover' persisted during the abnormal air-pollution episode

125   during December 5–9, 1952 in London as well as February 21-26, 2014 in Beijing. It is worth pointing out

126   that the bottom edge of 'warm cover' in the free troposphere declined day-by-day. During the heavy

127   pollution incident, the 'warm cover' dropped to 900 hPa (Figs. 1g and 1h). The above analysis shows that

128   in the ABL over London during December 5–9, 1952 and Beijing during February 21–26, 2014, the

129   inversion layer height decreased, which made the ABL structure stable for accumulation of air pollutants.

130   The deep 'warm cover' structures in the middle troposphere acted as a precursory 'strong signal' of the

131   Great Smog of London and Beijing's heavy air pollution.
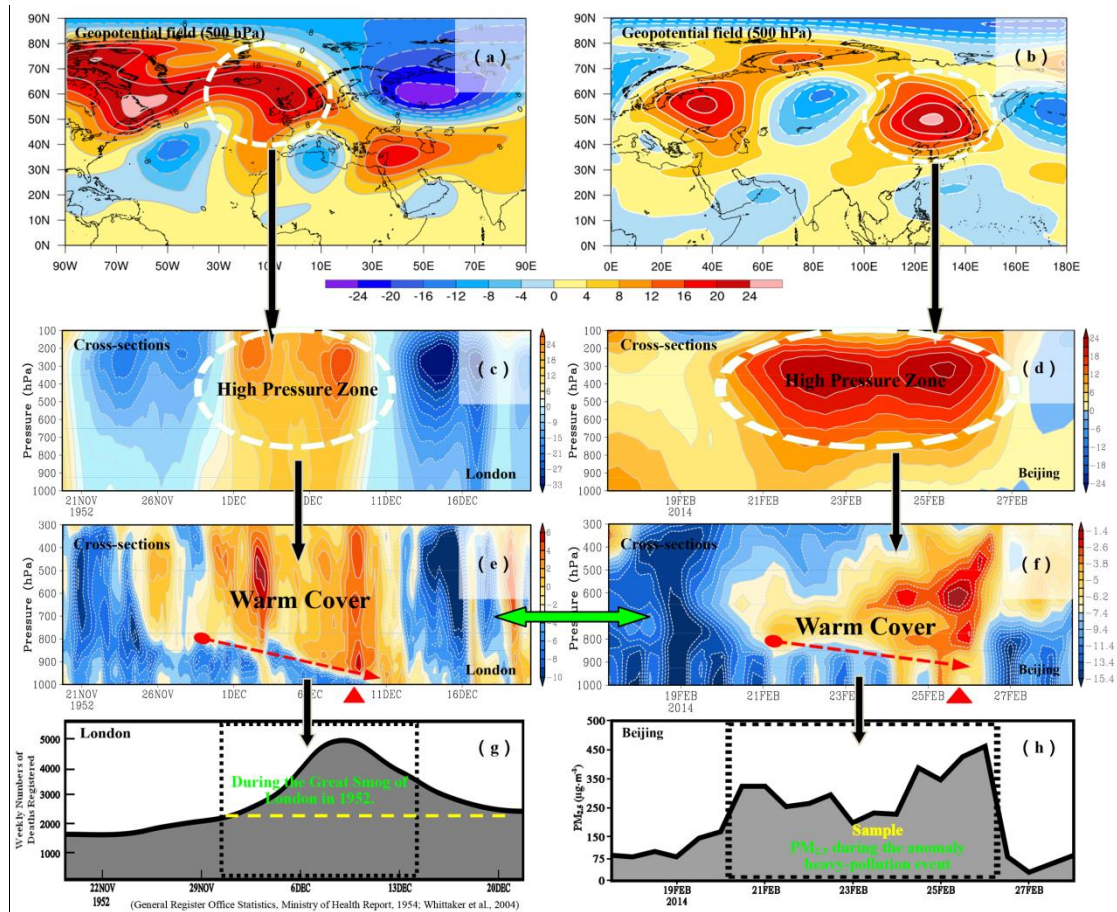
Figure 1. Dynamical and thermodynamical structures and air pollution variations: (a) geopotential height anomalies (unit: dagpm) at 500 hPa during December 5-9, 1952 for the Great Smog of London, (b) the same as (a) but during February 21-26, 2014. (c) Time-vertical cross-sections of the geopotential height anomalies (unit: dagpm) in the high pressure area (50-70 N; 20 W -10 E) during November 20 to December 20, 1952，(d) the same as (c) but in the high pressure area (40-63 N; 115-138 E) during February 17-28, 2014. (e) Time-vertical cross-sections of air temperature anomalies (unit: ℃) over London (the Red dotted arrow shows the bottom edge of the 'warm cover' during the Great Smog in London) during November 20 to December 20, 1952, (f) the same as (e) but during the heavy pollution in February 2014 over Beijing. (g) Weekly death rate in London prior to, during and after the 1952 pollution episode (General Register Office Statistics, Ministry of Health Report, 1954; Whittaker et al., 2004). (h) The variation of surface $PM_{2.5}$ concentrations (units: µg·m^{-3}) during the heavy pollution in February 2014 over Beijing.

3.2 Effect of 'Warm Cover' in the free troposphere on ABL and surface $PM_{2.5}$ variations

During five heavy air pollution episodes over Beijing in December 2015 and 2016 the vertical structures of air temperature anomalies presented the 'warm cover' structure in the free troposphere (see Fig. S1).

7

147 During winter 2014-2017, Figs. 2a and 2b demonstrated the significant negative correlations between the

148 height of the ABL and air temperature anomalies over same period and 24 hours ahead in Beijing, and the

149 correlation coefficients were 0.41 and 0.34 (99.9% confidence level), reflecting that the 'warm cover'

150 structure hidden in the middle troposphere with significant 'strong-signal' features is of persistent

151 premonitory significance for the heavy pollution episodes. Figs. 2c–2e presented the significant positive

152 correlations between $PM_{2.5}$ concentrations and air temperature anomalies over same period and 24, 48

153 hours ahead in Beijing, and the correlation coefficients were 0.42, 0.56 and 0.37 (99.9% confidence level).

154 Based on the above mentioned results, air temperature anomalies over 24 and 48 hours ahead could also

155 be reflected that 'warm cover' hidden in the middle troposphere could be regarded as the precursory

156 'strong-signal' for air pollution change. Furthermore, such a 'stable' structure also restricted the vertical

157 transport of moist air from the lower to the middle troposphere for forming secondary aerosols, which

158 could dominate $PM_{2.5}$ concentrations in air pollution over China (Huang et al., 2014; Tan et al., 2015).
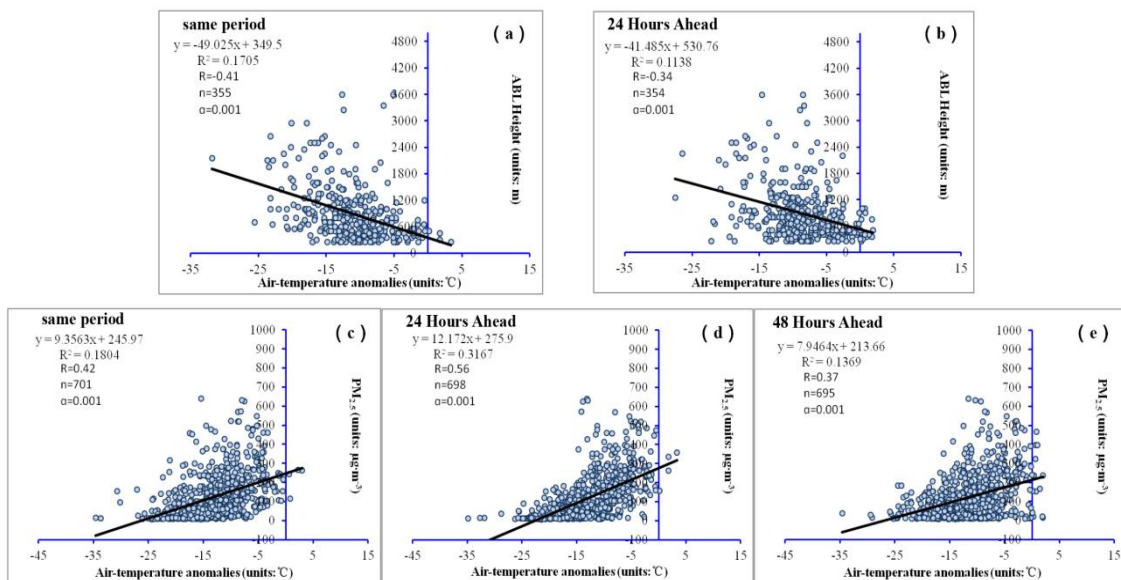
159

160 **Figure 2.** The correlations between ABL height and air temperature anomalies in Beijing during winter 2014–2017, (a) same

161 period, at 800 hPa; (b) 24 hours ahead, at 650 hPa. The correlations between $PM_{2.5}$ concentration and air temperature

162 anomalies in Beijing during winter 2014–2017, (c) same period, at 850 hPa; (d) 24 hours ahead, at 800 hPa; (e) 48 hours

163 ahead, at 724 hPa.

164

3.3 Changes of the 'warm cover' structure in the middle troposphere

The 'warm cover' structure of air temperature anomalies in the middle troposphere indicated the

intensification of heavy air pollution. The 'warm cover' structure is a precursory 'strong signal' for the

frequent occurrence of regional haze events. The air pollution in EC exhibited the significant seasonal

variations. Our study revealed that existed seasonal differences of the thermal structures in the atmosphere

over EC. In spring (Figs. 3a and 3e) and summer (Figs. 3b and 3f), the middle troposphere was

characterized by a 'upper cooling and bottom warming' vertical structure for less air pollution. When the

autumn (Figs. 3c and 3g) and winter (Figs. 3d and 3h) arrived, the middle troposphere was characterized by

a 'upper warming and bottom cooling' vertical structure, which intensified the air pollution. In autumn,

atmospheric thermal structure over EC was marked with a transition between summer and winter (Fig. 3c).

The atmosphere condition reversed in winter, a large-scale anomalous air temperature pattern of 'upper

warming and bottom cooling' in the middle troposphere appeared from the plateau to downstream EC

region and even the entire East Asian region (Fig. 3d). The structure of 'warm cover' in winter was much

stronger than that in autumn, and its height of the former was much lower than that of the latter. Therefore,

the intensity of air pollution over EC during winter is significantly higher than other seasons (Fig. 3h).

From the perspective of interdecadal variations, our study revealed a close relationship between the

frequent occurrence of haze events in EC and the atmospheric thermal structure in the eastern Tibetan

Plateau (TP). Furthermore, the thermal structures of the troposphere exhibited the distinct interdecadal

variations (Figs. 4a-4c). A cooling structure was identified in the wintertime air temperature anomalies over

the east region of TP during 1961−1980 (Fig. 4a); the upper level of the eastern TP during 1981−2000

showed a 'upper cooling and bottom warming' vertical structure (Fig. 4b). The interdecadal changes of

vertical structure reversed during 2001−2018 with a significant 'warm cover' (Fig. 4c). The years of 2001−

187   2018 witnessed the highest frequency of haze days (Fig. 4f), and 1981–2000 saw a middle-level occurrence

188   of haze days (Fig. 4e), while the lowest frequency of haze days occurred during 1961–1980 (Fig. 4d).

189   The concept of variations of the tropospheric 'warm cover' has been proposed in this work. Under the

190   background of climate change, it is worth considering whether the variational tendency of the structure of

191   the plateau's heat source induces variations of the tropospheric thermal structure in downstream areas of the

192   Plateau, leading to the interdecadal variations of the frequency of haze events seen in Eastern China since

193   the 21th century. Thermal anomalies of the TP also play an important role in the variations of the frequency

194   of haze events in EC apart from the anthropogenic pollutant emission related to the rapid industrialization

195   of China. The observational and modeling studies have demonstrated that the interannual variations in the

196   thermal forcing of TP are positively correlated with the incidences of wintertime haze over EC (Xu et al.,

197   2016). The TP induced changes in atmospheric circulation, increasing atmospheric stability and driving

198   frequent haze events in EC (Xu et al., 2016). In this study, the data analysis concerning the interannual

199   variations of the TP's apparent heat source and air temperature in wintertime at the TP with the altitudes

200   above 3000 meters showed that since the 1960s the heat source in areas vulnerable to TP climate change

201   strengthen continuously as the surface temperature increased (Fig. 5a). Furthermore, the TP's apparent heat

202   and air temperature of the middle troposphere over EC presented the significant positive correlation passing

203   (90% confidence level), which is similar to 'warm cover' structures (Fig. 5b). Therefore, we considered that

204   the 'warm cover' change in the middle troposphere over EC was closely related to TP's apparent heat and

205   the surface temperature. The TP induced changes in thermodynamic structure of atmospheric provided

206   favorable climatic backgrounds driving air pollution events in EC.

207
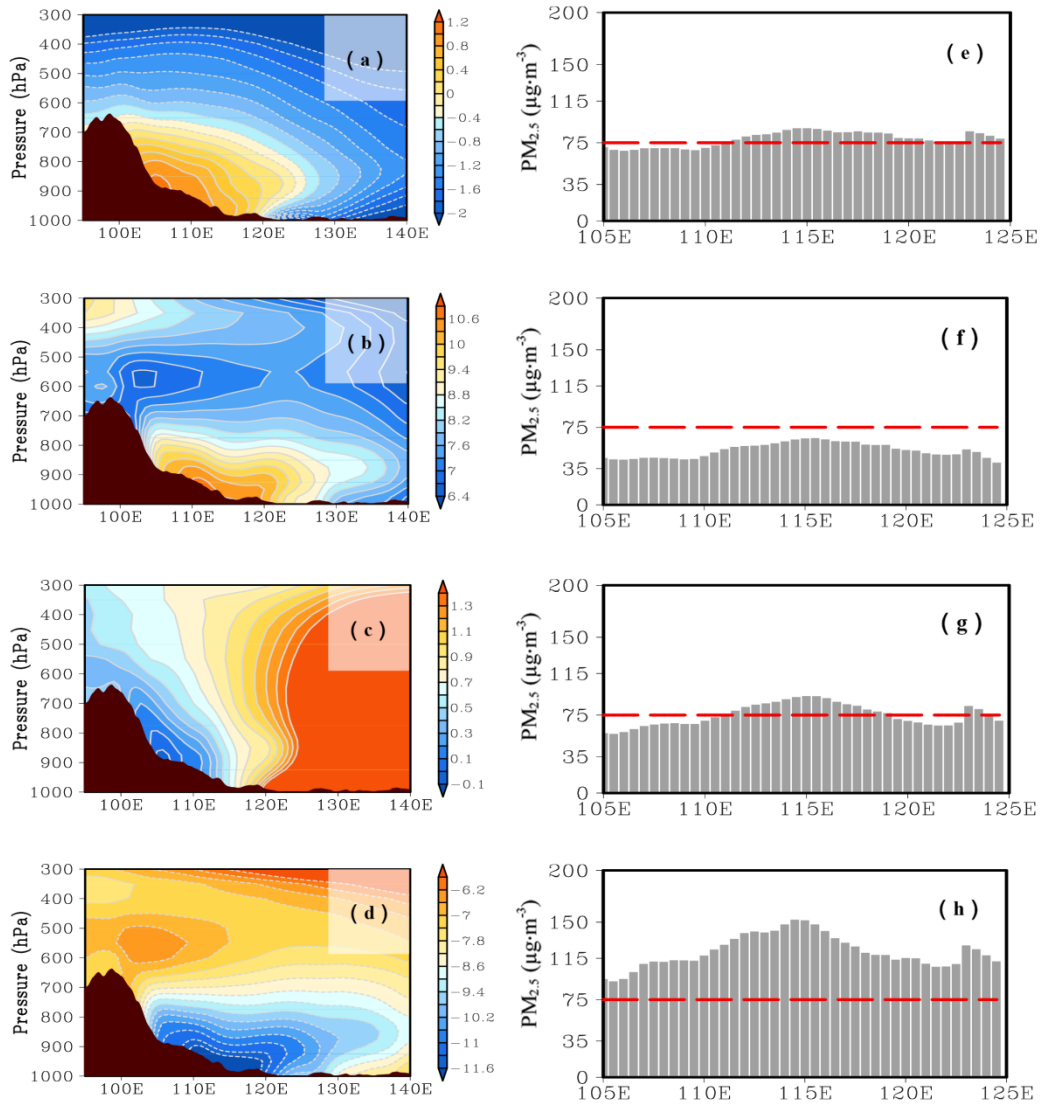
Figure 3. Vertical cross sections of (a-d) air temperature anomalies (unit: ℃) and (e-h) the PM$_{2.5}$ concentrations (unit: μg·m^{-3})
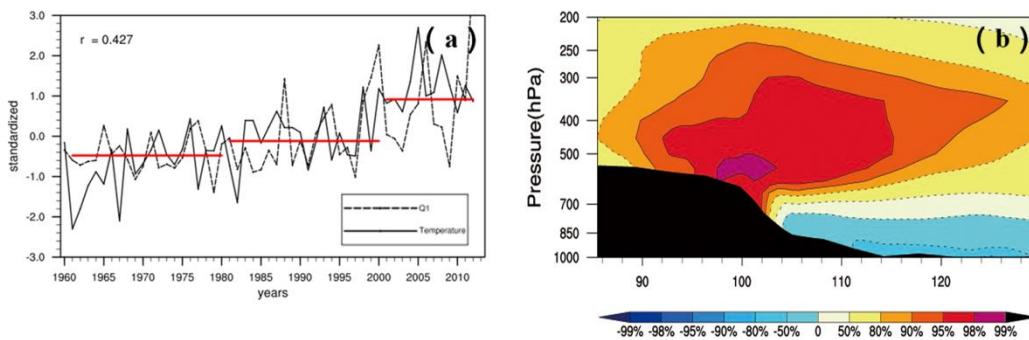
averaged along 25-40 N in spring (a, e), summer (b, f), autumn (c, g), winter (d, h) from 2013 to 2018.
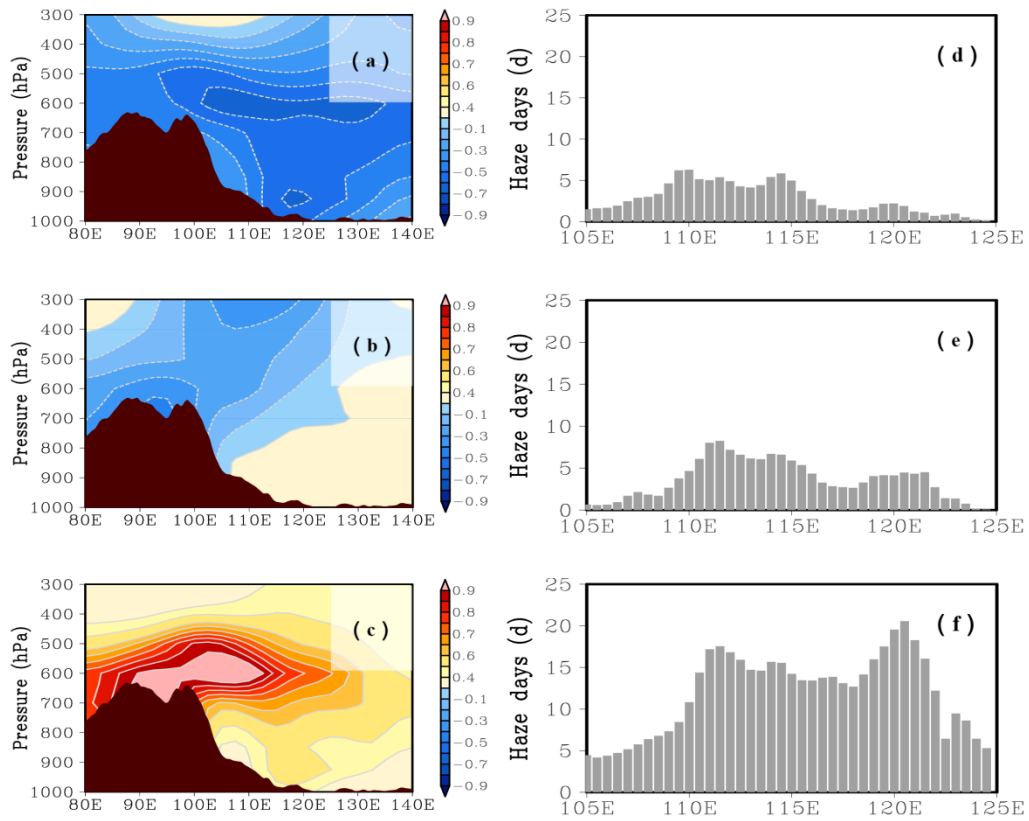
Figure 4. Vertical cross sections of (a-c) air temperature anomalies (unit: ℃) and (d-f) the number of haze days averaged along 25-40 °N in winter during 1961-1980 (a, d), 1981-2000 (b, e) and 2001-2018 (c, f).

Figure 5. (a) Interanual variations of TP's apparent heat source (Q_1) and air temperature of meteorological stations in the TP with the altitudes above 3000 meters in the winters during 1960-2014; (b) Vertical cross sections of the correlations between TP's apparent heat (Q_1) and air temperature latitude-averaged along 30-35 °N in the winters during 1960-2014.

4 Conclusions and discussion

Based on the study of the Great Smog of London in 1952 and Beijing's heavy air pollution in 2014, as well

12

221   as $PM_{2.5}$ pollution over EC, the anomalous 'warm cover' in the middle troposphere was identified as a

222   precursory 'strong signal' for severe air pollution events, which could be attributed to climate change. A

223   stable thermal structure in the middle troposphere, i.e. a 'warm cover', suppressed the ABL development,

224   which was a key 'inducement' for the accumulation of air pollutants in the ambient atmosphere.

225   From the perspective of the thermal vertical structure in the troposphere, the abnormal vertical

226   structure in the troposphere during heavy air pollution were understood in this study. The thermal structure

227   formed by the conventional decline rate of atmospheric air temperature often 'covers up' the anomalous

228   'strong signal' of the troposphere in air pollution process, such as the abnormal stable structure with the

229   middle warm and bottom cold in the troposphere with air temperature anomalies. The 'strong signal' of the

230   'warm cover' of air temperature anomalies in the middle troposphere during heavy air pollution can be

231   described by the method of statistical comprehensive diagnosis analysis.

232   A large-scale anomalous air temperature pattern of 'upper warming and bottom cooling' in the

233   troposphere appeared from the TP to the downstream EC region and even the entire East Asian region. The

234   frequent haze pollution events in EC since the start of the 21st century happens to be within a significant

235   positive phase in the interdecadal variations of 'warm cover' in the middle troposphere. A close relationship

236   between the TP's heat and the thermal structure in the atmosphere in EC and even the entire East Asian

237   region reflected an important role of TP's thermal forcing in environment change over China.

238

239   *Data availability.* The monthly NCEP/NCAR reanalysis data of meteorology are collected from the U.S.

240   National Center for Environmental Protection (NCEP, https://www.esrl.noaa.gov/); the daily and monthly

241   ERA-Interim reanalysis data of meteorology are collected from the European Center for Medium-range

242   Weather Forecasts (ECMWF, https://www.ecmwf.int/); the hourly $PM_{2.5}$ concentration data are collected

243 from the national air quality monitoring network operated by the Ministry of Ecology and Environment the

244 People's Republic of China (http://www.mee.gov.cn/); the air temperature of surface observation data and

245 L-band sounding data are obtained from the China Meteorological Information Center (http://data.cma.cn/).

246 All data presented in this paper are available upon request to the corresponding author (Wenyue Cai,

247 caiwy@cma.gov.cn).

248

249 *Author contributions.* XDX and WYC designed the study. XDX, WYC and TLZ performed the research.

250 WYC performed the statistical analyses. XDX, WYC and TLZ wrote the initial paper. TLZ, XFQ, WHZ,

251 CS, PY, CZW and FG contributed to subsequent revisions.

252

253 *Competing interests.* The authors declare that they have no conflict of interest.

254

262

263 **References**

264 Cai, M., OU, J. J., Zhou, Y. Q., Yang Q., and Cai, Z. X.: Discriminating cloud area by using L-band
265   sounding data (in Chinese), Chin. J. Atmos. Sci., 38, 213–222,
266   https://doi.org/10.3878/j.issn.1006-9895.2013.12193, 2014.

267 Cai, W. Y., Xu, X. D., Cheng, X. H., Wei, F. Y., Qiu, X. F., and Zhu, W. H.: Impact of "blocking" structure

268   in the troposphere on the wintertime persistent heavy air pollution in northern China, Sci. Total

269   Environ., 741, 140325, https://doi.org/10.1016/j.scitotenv.2020.140325, 2020.

270 Cheng, Y. F., Zheng, G. J., Wei, C., Mu, Q., Zheng, B., Wang, Z. B., Gao, M., Zhang, Q., He, K. B.,

271   Carmichael, G., Poschl, U., and Su, H.: Reactive nitrogen chemistry in aerosol water as a source of

272   sulfate during haze events in China, Sci. Adv., 2, e1601530, https://doi.org/10.1126/sciadv.1601530,

273   2016.

274 China Ministry of Environmental Protection: Technical Regulation on Ambient Air Quality Index (On Trial)

275   (HJ633-2012), China Environmental Science Press, Beijing, China, 2012.

276 Ding, Y. H. and Liu, Y. J.: Analysis of long-term variations of fog and haze in China in recent 50 years and

277   their relations with atmospheric humidity, Science China: Earth Sciences, 57, 36-46,

278   https://doi.org/10.1007/s11430-013-4792-1, 2014.

279 Huang, R. J., Zhang, Y., Bozzetti, C., Ho, K. F., Cao, J. J., Han, Y. M., Daellenbach, K. R., Slowik, J. G.,

280   Platt, S. M., Canonaco, F., Zotter, P., Wolf, R., Pieber, S. M., Bruns, E. A., Crippa, M., Ciarelli, G.,

281   Piazzalunga, A., Schwikowski, M., Abbaszade, G., Schnelle-Kreis, J., Zimmermann, R., An, Z. S.,

282   Szidat, S., Baltensperger, U., Haddad, I. E., 11, and Prevot, A-S. H.: High secondary aerosol

283   contribution to particulate pollution during haze events in China, Nature, 514, 218–222,

284   https://doi.org/10.1038/nature13774, 2014.

285 Li, W., Li, F., Zhao, Z. Q., Liu, F. Q., Li, B., Li, H.: L-Band Meteorological Observation System

286   Construction Technology Assessment Report (in Chinese), China Meteorological Press, Beijing, China,

287   2009.

288 Liu, S. Y. and Liang, Z. X.: Observed diurnal cycle climatology of planetary boundary layer height, J.

289   Climate, 23, 5790-5809, https://doi.org/10.1175/2010JCLI3552.1, 2010.

290 Miao, Y. C., Li, J., Miao, S. G., Che, H. Z., Wang, Y. Q., Zhang, X. Y., Zhu, R., and Liu, S. H.: Interaction

291   Between Planetary Boundary Layer and $PM_{2.5}$ Pollution in Megacities in China: a Review. Current

292   Pollution Reports, 5, 261–271, https://doi.org/10.1007/s40726-019-00124-5, 2019.

293   Quan, J. N., Gao, Y., Zhang, Q., Tie, X. X., Cao, J. J., Han, S. Q., Meng, J. W., Chen, P. F., and Zhao, D. L.:

294   Evolution of planetary boundary layer under different weather conditions, and its impact on aerosol

295   concentrations, Particuology, 11(1), 34-40, https://doi.org/10.1016/j.partic.2012.04.005, 2013.

296   Quan, J. N., Xu, X. D., Jia, X. C., Liu, S. H., Miao, S. G., Xin, J. Y., Hu, F., Wang, Z. F., Fan, S. J., Zhang,

297   H. S., Mu, Y. J., Dou, Y. W., and Cheng, Z.: Multi-scale processes in severe haze events in China and

298   their interactions with aerosols: Mechanisms and progresses (in Chinese). Chin Sci Bull, 65, 810–824,

299   https://doi.org/10.1360/TB-2019-0197, 2020.

300   State Council of the People's Republic of China: Notice of the General Office of the State Council on

301   Issuing the Air Pollution Prevention and Control Action Plan, State Council of the People's Republic

302   of China website. Available at: http://www.gov.cn/zwgk/2013-09/12/content_2486773.htm, 2013.

303   State Council of the People's Republic of China: Notice of the General Office of the State Council on

304   Issuing the Air Pollution Prevention and Control Action Plan, State Council of the People's Republic

305   of China website. Available at: http://www. gov.cn/zhengce/content/2018-07/03/content_5303158.htm.

306   2018.

307   Tan, C. H., Zhao, T. L., Cui, C. G., Luo, B. L., and Bai, Y. Q.: Characterization of haze pollution over

308   Central China during the past 50 years, Science in China (in Chinese), China Environ. Sci., 35, 2272–

309   2280, 2015.

310   Tang, G. Q., Zhang, J. Q., Zhu, X. W., Tao, S., Munkel, C., Hu, B., Schaefer, K., Liu, Z. R., Zhang, J. K.,

311   Wang, L. L., Xin, J. Y., Schaefer, P., and Wang, Y. S.: Mixing layer height and its implications for air

312   pollution over Beijing, China, Atmos. Chem. Phys., 16, 2459–2475,

313   https://doi.org/10.5194/acp-16-2459-2016, 2016.

314   Tie, X. X. and Cao, J. J.: Aerosol pollutions in eastern China: Present and future impacts on environment,

315   Particuology, 7, 426–431, https://doi.org/10.1016/j.partic.2009.09.003, 2009.

316   Wang, G. H., Zhang, R. Y., Gomez, M. E., Yang, L. X., Zamora, M. L., Hu, M., Lin, Y., Peng, J. F., Guo, S.,

Meng, J. J., Li, J. J., Cheng, C. L., Hu, T. F., Ren, Y. Q., Wang, Y. S., Gao, J., Cao, J. J., An, Z. S., Zhou, W. J., Li, G. H., Wang, J. Y., Tian, P. F., Marrero-Ortiz, W., Secrest, J., Du, Z. F., Zheng, J., Shang, D. J., Zeng, L. M., Shao, M., Wang, W. G., Huang, Y., Wang, Y., Zhu, Y. J., Li, Y. X., Hu, J. X., Pan, B., Cai, L., Cheng, Y. T., Ji, Y. M., Zhang, F., Rosenfeld, D., Liss, P. S., Duce, R. A., Kolb, C. E., and Molina, M. J.: Persistent sulfate formation from London Fog to Chinese Haze, P. Natl. Acad. Sci., 113, 13630–13635, https://doi.org/10.1073/pnas.1616540113, 2016.

Wang, H., Li, J. H., Peng, Y., Zhang, M., Che, H. Z., and Zhang, X. Y.: The impacts of the meteorology features on $PM_{2.5}$ levels during a severe haze episode in central-east China, Atmospheric Environment, 197, 177–189, https://doi.org/10.1016/j.atmosenv.2018.10.001, 2019.

Wang, H., Xue, M., Zhang, X. Y., Liu, H. L., Zhou, C. H., Tan, S. C., Che, H. Z., Chen, B., and Li, T.: Mesoscale modeling study of the interactions between aerosols and PBL meteorology during a haze episode in Jing–Jin–Ji (China) and its nearby surrounding region – Part 1: Aerosol distributions and meteorological features, Atmos. Chem. Phys., 15, 3257–3275, https://doi.org/10.5194/acp-15-3257-2015, 2015.

Wang, J. J., Zhang, M. G., Bai, X. L., Tan, H. J., Li, S., Liu, J. P., Zhang, R., Wolters, M. A., Qin, X. Y., Zhang, M. M., Lin, H. M., Li, Y. N., Li, J., and Chen, L. Q.: Large-scale transport of $PM_{2.5}$ in the lower troposphere during winter cold surges in China, Sci. Rep., 7, 13238, https://doi.org/10.1038/s41598-017-13217-2, 2017.

Wang, Y. S., Li, W. J., Gao, W. K., Liu, Z. R., Tian, S. L., Shen, R. R., Ji, D. S., Wang, S., Wang, L. L., Tang, G. Q, Song, T., Cheng, M. T., Wang, G. H., Gong, Z. Y., Hao, J. M., and Zhang, Y. H.: Trends in particulate matter and its chemical compositions in China from 2013–2017. Science China Earth Sciences, 62: 1857–1871, https://doi.org/10.1007/s11430-018-9373-1, 2019.

Whittaker, A., Berube, K., Jones, T., Maynard, R., Richards, R.: Killer smog of London, 50 years on: particle properties and oxidative capacity, Science of the Total Environment, 334-335, 435–445, https://doi.org/10.1016/j.scitotenv.2004.04.047, 2004.

Xu, X. D., Zhao, T. L., Liu, F., Gong, S. L., Kristovich, D., Lu, C., Guo, Y., Cheng, X. H, Wang, Y. J., and Ding, G.: Climate modulation of the Tibetan Plateau on haze in China, Atmos. Chem. Phys., 16, 1365–1375, https://doi.org/10.5194/acp-16-1365-2016, 2016.

Yim, S-Y., Wang, B., Liu, J., and Wu, Z. W.: A comparison of regional monsoon variability using monsoon indices, Climate Dynamics, 43, 1423-1437, https://doi.org/10.1007/s00382-013-1956-9, 2014.

347 Zhang, X. Y., Wang, J. Z., Wang, Y. Q., Liu, H. L., Sun, J. Y., and Zhang, Y. M.: Changes in chemical
348   components of aerosol particles in different haze regions in China from 2006 to 2013 and contribution
349   of meteorological factors, Atmos. Chem. Phys., 15, 12935–12952,
350   https://doi.org/10.5194/acp-15-12935-2015, 2015.
351 Zhu, W. H., Xu, X. D., Zheng, J., Yan, P., Wang, Y. J., and Cai, W. Y.: The characteristics of abnormal
352   wintertime pollution events in the Jing-Jin-Ji region and its relationships with meteorological factors,
353   Sci. Total Environ., 626, 887-898, https://doi.org/10.1016/j.scitotenv.2018.01.083, 2018.